applied sciences

MDPI

Article

Development and Testing of an Active Noise Control System for Urban Road Traffic Noise

Biyu Yang [1,2], Jiacun Yin [3], Zhoujing Ye [3], Songli Yang [3] and Linbing Wang [4,*]

1 Highway School, Chang'an University, Xi'an 710054, China; yang.yby@gmail.com
2 Zhaotong Highway Investment Development Co., Ltd., Zhaotong 657099, China
3 National Center for Materials Service Safety, University of Science and Technology Beijing, Beijing 100083, China; jcyin11@163.com (J.Y.); yezhoujing@ustb.edu.cn (Z.Y.); songliyang96@gmail.com (S.Y.)
4 School of Environmental, Civil, Agricultural and Mechanical Engineering, University of Georgia, Athens, GA 30602, USA
* Correspondence: linbing.wang@uga.edu

Abstract: As urbanization accelerates, the increasing number of vehicles and travel demands contribute to escalating road traffic noise pollution. Although passive noise control techniques such as noise barriers and green belts effectively mitigate noise, they occupy urban space, exacerbating the scarcity and high cost of already congested city areas. Emerging as a novel noise reduction strategy, active noise control (ANC) eliminates the need for physical isolation structures and addresses the noise within specific frequency ranges more effectively. This paper investigates the characteristics of urban road traffic noise and develops an ANC prototype. Utilizing the Least Mean Squares (LMS) algorithm, we conduct active noise control tests for various types of single- and dual-frequency noise within the prototype's universal platform to validate its actual noise reduction capabilities. The study demonstrates that urban road traffic noise is mostly in the mid- to low-frequency range (below 2000 Hz). The developed ANC prototype significantly reduces single- or dual-frequency noise within this range, achieving a maximum noise reduction of nearly 30 dB(A). Future research should expand noise reduction tests across more frequency bands and assess the noise reduction effectiveness against real road traffic noise.

Keywords: road traffic noise; active noise control; prototype system; LMS algorithm; single- and dual-frequency tests

check for updates

Citation: Yang, B.; Yin, J.; Ye, Z.; Yang, S.; Wang, L. Development and Testing of an Active Noise Control System for Urban Road Traffic Noise. *Appl. Sci.* **2024**, *14*, 175. https://doi.org/10.3390/app14010175

Academic Editor: Tao Zhu

Received: 16 October 2023
Revised: 10 December 2023
Accepted: 13 December 2023
Published: 25 December 2023

1. Introduction

With the development of urbanization, road traffic noise has become the main source of urban noise pollution, accounting for 60–80% [1]. Noise exceeding 50 dB affects sleep and rest, noise exceeding 70 dB triggers psychological stress and distraction, and living for a long time in a noise environment of more than 90 dB can seriously damage hearing and induce other health problems [2]. Therefore, it is necessary to explore effective road traffic noise reduction techniques to curb road traffic noise pollution.

Currently, passive noise control techniques, such as constructing sound barriers on the roadside, are mainly used to reduce the impact of road traffic noise on people's living areas, but the sound barriers not only obstruct the line of sight but also fail to reduce specific-frequency noise [3,4]. In addition, by changing the texture of the road surface, the selection of porous pavement materials and other means can effectively reduce the high-frequency part of the traffic noise, but the low-frequency noise reduction effect is poor [5–9].

Active noise control (ANC) reduces or eliminates unwanted environmental noise by generating sound waves that are opposite to the external noise [10]. Currently, active noise control techniques have been extensively researched and applied in hoods, headphones, pipelines, transformers, mines, and magnetic resonance imaging equipment [11–18]. In the field of road traffic, active noise control technology is widely used in vehicle noise control: Xu Gege et al. used a convolutional neural network to classify road surfaces, improving the vehicle noise reduction by adjusting the LMS algorithm based on the road type [19]. Feng et al. experimented with using ANC inside vehicles, using algorithms like TF-FxLMS and SFxLMS to lower the computational efforts and compare the algorithm complexities [20]. Zhang et al. developed a multichannel adaptive algorithm to control the engine noise in vehicles, especially those with prominent harmonic noise [21]. Jiang's group enhanced the SPSA algorithm for ANC in vehicles, targeting low-frequency noise near the driver's head, reducing the interior noise by an average of 10 dB [22]. Zhang proposed a method for grouping virtual reference signals in vehicle road noise control systems, cutting the computational complexity by about 24.4% and reducing noise by up to 4.48 dB in the roar frequency band [23].

The current active noise control technology has a good noise reduction effect in closed space environments, but the noise reduction effect in open space environments with multiple sound sources needs to be improved [24]. As road traffic noise is affected by many factors such as traffic flow, speed, and vehicle position, it is non-stationary noise, and vehicles are mobile sound sources with a Doppler effect. It is much more difficult to achieve active noise control in a spacious open environment than in a closed space [25].

Controlling roadside traffic noise with active noise control (ANC) techniques presents significant challenges. Researchers have explored various solutions, focusing on different aspects of noise control in real-world settings. One approach is to use ANC in confined spaces like tunnels. For instance, Zhang developed an ANC device for highway tunnels, achieving up to 10.48 dB noise reduction, though the test was limited to a fixed noise source [26]. Moon H. R. et al. expanded on this by testing an ANC device in a tunnel model with a more complex noise source, showing a reduction of 4–15 dB [27].

However, in typical road traffic environments, the noise from moving vehicles is often distant from ANC systems, leading to unstable signals. To address this, Zhao et al. proposed using a fixed coefficient feedforward ANC system with a pseudo-noise source, demonstrating the feasibility of this approach [28]. Combining active and passive noise reduction techniques has also been explored. Lam et al. showed that mounting ANC systems onto sound barriers can significantly cut down the low-frequency noise [29,30]. Similarly, Denis et al. combined sound barriers with ANC systems to identify effective noise reduction strategies, including the placement and number of microphones and secondary sound sources [31]. Tire–road noise is another area of focus. Sahib et al. suggested installing ANC systems near the tire–road contact point, acknowledging the challenges and research needs with this method [32]. Zhang et al. explored the effect of ANC in small openings, finding that effective broadband noise control is possible even in limited spaces [33].

In summary, applying active noise control (ANC) to roadside traffic noise is challenging and currently at the research stage. This paper aims to advance the application of ANC in this field. Our approach includes analyzing the road traffic noise characteristics and developing an ANC prototype system. This development involved optimizing the noise reduction algorithm parameters, understanding the ANC principles, and selecting the appropriate software and hardware. We also conducted extensive tests on single-frequency, dual-frequency, and real traffic noise. The results of these tests provide valuable technical insights for implementing ANC in roadside noise control.

2. Characterization of Road Traffic Noise

2.1. Traffic Noise Collection

To understand the variation laws of road traffic noise in terms of frequency, intensity, time, and different spaces, the UMIK-1 measuring microphone with a built-in sound card was used in this experiment, and the overall road traffic noise was measured using the roadside method. The test process refers to Sound environment quality Standard GB3096-2008 [34] and Technical specifications for environmental noise monitoring Routine monitoring for urban environmental noise HJ640-2012 [35]. At each monitoring point, the UMIK-1 microphone is used to collect the sound intensity of the road traffic noise for 20 min continuously, that is, the curve of the sound pressure amplitude varying with time.

Five test points were set up in the road network of Beijing; the points were selected on the side of the road and on the pedestrian bridge of the straight section to avoid the interference of intersections, traffic lights, fixed sound sources, crowds, reflectors, and other influencing factors. The distance between the microphone and the roadside was 20 cm, and the vertical distance between the microphone and the road was 1.5 m. The specific location and environmental parameters of the test points are shown in Figure 1.

Sites	Temperature	Wind	Distance from Roadside	Height above Road Surface
1	8 °C	Southeast wind 3m/s	3.5 m	1.5 cm
2	9 °C	Southeast wind 4m/s	20 cm	1.5 m
3	12 °C	Southwest wind 2m/s	0 m	6 m
4	14 °C	Southwest wind 1m/s	20 cm	1.5 m
5	9 °C	Northeast wind 2m/s	20 cm	1.5 m

Figure 1. Road traffic noise testing setup and locations, temperature, wind, distance, and height from road.

After the road traffic noise is collected using the UMIK-1 measuring microphone, the Smaart v8 software is used to analyze the data. The manufacturer of the UMIK-1 measuring microphone is miniDSP, a technology company in Hong Kong. This microphone has a frequency response range of 20 Hz–20 kHz and a sampling rate of 48 kHz. It is a 6 mm electret omnidirectional microphone. The Smaart v8, developed by an acoustic test and measurement company called Rational Acoustics LLC in Woodstock, CT, USA, is a widely used tool for audio measurement and analysis. This paper uses the latest version, smaart v8. In order to analyze the frequency distribution law of road traffic noise, the frequency spectrum of the noise is analyzed.

2.2. Noise Characteristics Analysis

2.2.1. Overall Traffic Noise Analysis

Continuously collecting 20 min of road traffic noise, recording various noise events, reflects the overall noise level of specific road sections or areas. This allows for an assessment of the short-term and long-term impact of traffic noise on the surrounding environment and community, enabling the implementation of corresponding noise reduction measures. Road traffic noise typically covers a wide frequency range as it comprises various sound sources, including noise from car engines, braking, tire–road contact, car horns, and aerodynamic resistance. These sound sources have different frequency ranges. Low-frequency noise typically falls within the range of 20 Hz to 200 Hz, usually including noise from large vehicle engines. Mid-frequency noise ranges from approximately 200 Hz to 2000 Hz, encompassing tire–road contact noise and noise from some vehicle engines. High-frequency noise primarily exists between 2000 Hz and 20,000 Hz and is mainly composed of car horns and braking noise [36–39]. Conducting a spectrum analysis of the overall noise allows for the reflection of the amalgamation of all noise sources, accounting for various vehicle types, traffic flows, and vehicle speeds. Figure 2 illustrates the overall noise levels at five testing points and the spectrum analysis within the 1/3 octave frequency bands.

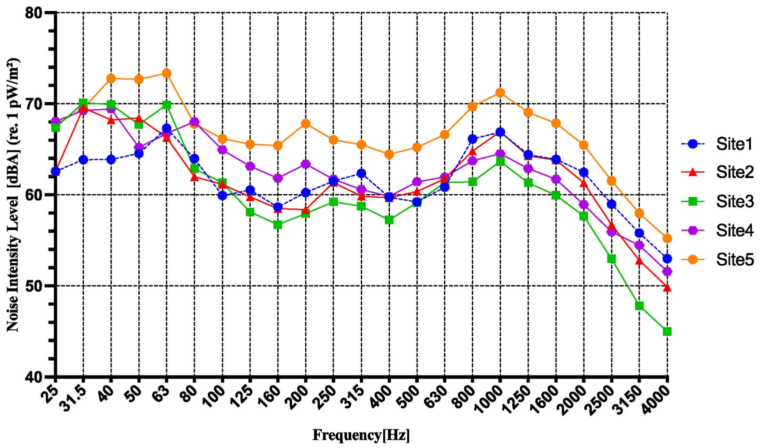

Figure 2. Noise levels and spectrum chart at test points.

The results indicate that vehicle speed may be a significant factor affecting the magnitude of road traffic noise. The vehicle speed on the secondary high-speed service road of the airport (Site5) is evidently higher than that at Site2, Site3, and Site4, and correspondingly, its noise level is also noticeably higher than these three sections. The vehicle speed at Site1 is also fast, but the measurement point is too far away for a direct comparison. Analysis of the noise spectrum reveals that while the spectral characteristics of different road sections generally follow the same trend, variations do exist. Peaks in the noise spectrum were observed at frequencies ranging from 50 to 80 Hz, 200 to 315 Hz, and 800 to 1250 Hz across the five testing sites. This primarily occurs due to the diverse types of vehicles and noise sources at each test point, leading to the manifestation of multi-peak characteristics in the frequency spectrum. Furthermore, at Site2, Site3, and Site4, there is a prevalence of lower-frequency noise in the range of 20 Hz to 200 Hz, surpassing the high-frequency noise between 200 Hz and 2000 Hz. This discrepancy can be attributed to the fact that these three test points are either auxiliary roads or urban expressways, where a significant number of vehicles such as electric vehicles, buses, and trucks, known to produce lower-frequency noise, pass through. In contrast, Site1 and Site5 represent urban high-speed roads where the predominant vehicles are small cars with higher speeds, resulting in fewer low-frequency noise sources. All test points exhibit peak effects in the range of 800 to 1250 Hz, mainly due to the friction noise between tires and road surfaces. Faster vehicle speeds lead to more pronounced effects of tire and road surface friction noise, explaining why Site5, the airport expressway, experiences significantly higher noise levels in this frequency range compared to the other test points.

The above test results indicate that the type of vehicle and its speed have a significant impact on the generation of traffic noise. Therefore, an active noise control system may need to incorporate vehicle characteristic recognition capabilities to generate matching anti-noise based on the specific characteristics and speeds of different vehicles. Alternatively, it may focus on controlling the noise within a certain frequency range that is produced by various types of vehicles, such as the peak noise within the range of 800 to 1250 Hz.

2.2.2. Noise Characterization of Different Types of Vehicles

In response to continuously collected road traffic noise, noise data from different types of vehicles passing by were extracted. Noise characteristics such as frequency, duration, and intensity were analyzed. This allows for a more precise analysis and assessment of the impact of individual vehicles on the overall noise level of the road section. For an individual vehicle, the speed at the measurement point significantly influences the noise generation. The experimental method in this study recorded a relatively concentrated distribution of vehicle speeds. Therefore, building upon the experiments and drawing from tests conducted by the U.S. Federal Highway Administration [40], research was conducted to supplement and investigate vehicle noise data under different vehicle types and speeds. The vehicle types were classified based on the categorization by the U.S. Federal Highway Administration into large, medium, and small vehicles. Large vehicles mainly refer to trucks and buses, medium vehicles include sedans and SUVs, while small vehicles encompass compact cars and motorcycles [41]. Figure 3 presents the noise spectrum of different vehicle types at various driving speeds.

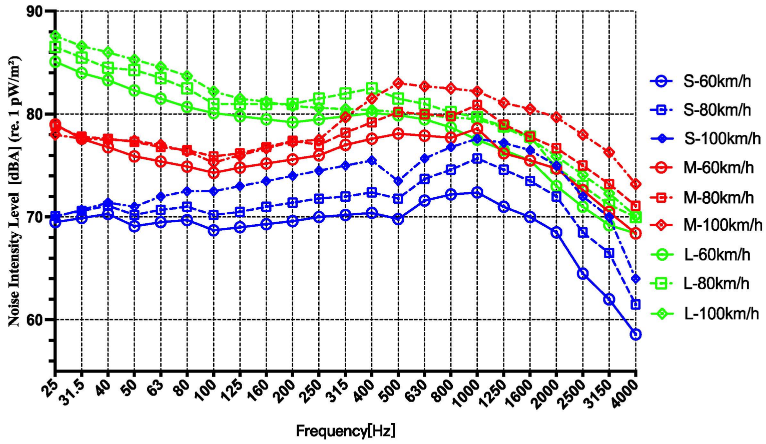

Figure 3. The spectrum of traffic noise at different vehicle speeds for three vehicle categories: small vehicles, medium vehicles, and large vehicles.

The above results indicate significant differences in the noise characteristics among small, medium, and large vehicles. Vehicle noise primarily originates from the engine, exhaust, the contact between the tires and the road surface, and aerodynamic noise. When comparing different speeds, at low speeds, the noise from motor vehicles is predominantly engine noise, while at high speeds, tire noise becomes the primary contributor [42]. Consequently, as the vehicle speed increases, the sound energy of noise shifts toward higher frequencies. However, the influence of speed on the noise frequency is limited, with the vehicle type having a pronounced impact. In terms of the effect of the vehicle type on noise frequency, in the low-frequency range (20–200 Hz), the noise in this frequency band is mainly composed of engine noise and mechanical vibrations. Small vehicles typically have smaller engines and lighter body structures, resulting in lower noise levels for small vehicles, while larger vehicles generate more significant vibrations and engine noise [43]. In the 200–2000 Hz frequency range, the aerodynamic noise generated by vehicles relative to air movement during travel is most pronounced. As vehicle speed increases, the corresponding aerodynamic noise also rises. Due to the typically superior body structure and aerodynamic design of medium and large vehicles compared to small vehicles, they may produce less aerodynamic noise during high-speed driving [44]. In contrast, smaller vehicles exhibit a more noticeable increase in noise within this frequency range as speed rises. In the 1000–4000 Hz frequency range, tire and road surface friction noise may predominantly occur. Medium and large vehicles often have greater weight and a larger contact area with the road surface, leading to stronger interactions with the road surface and, consequently, higher tire-road contact noise within this frequency range.

Moreover, different types of vehicles generate noise with energy concentrated in varying frequency ranges. When the driving speed exceeds 40 km/h, the peak center frequency of the noise from small cars is 1000 Hz, with energy primarily concentrated in the 600–2000 Hz range. The noise from medium-sized vehicles has a peak center frequency at 500 Hz, with energy mainly distributed within 2000 Hz. For large vehicles, the peak center frequency is 63 Hz, with the majority of energy spread under 1000 Hz. Research has shown that on highways with a high proportion of large freight vehicles, low-frequency noise is more prominent, with the sound energy mostly distributed around 400 Hz [45,46]. Therefore, when formulating noise reduction strategies, it is essential to refer to the actual noise characteristics of the target area and determine the frequency range where energy is primarily concentrated.

3. Development of the Active Noise Control Prototype System

3.1. Principles of Active Noise Control

Active noise control (ANC) is a potent noise reduction technology, operating on the principle of sound wave interference; that is, when two sound waves overlap at the same spatial location, they interact with each other based on the principle of superposition [47]. ANC achieves noise reduction by generating a secondary noise source with equal amplitude and opposite phase to the original noise source, thereby causing them to cancel each other out and effectively reducing the noise level.

This process can be expressed mathematically. If the phases of two sound waves of the same frequency at a certain location in space are φ_1 and φ_2, their sound pressure amplitude values are:

$$\begin{cases} p_1 = p_{1a}\cos(\omega t - \varphi_1) \\ p_2 = p_{2a}\cos(\omega t - \varphi_2) \end{cases} \tag{1}$$

According to the principle of superposition, the total sound pressure is the sum of their individual sound pressures:

$$p = p_1 + p_2 = p_{1a}\cos(\omega t - \varphi_1) + p_{2a}\cos(\omega t - \varphi_2) = p_a\cos(\omega t - \varphi) \tag{2}$$

where,

$$\begin{cases} p_a^2 = p_{1a}^2 + p_{2a}^2 + 2p_{1a}p_{2a}\cos(\varphi_2 - \varphi_1) \\ \varphi = arctan\frac{p_{1a}sin\varphi_1 + p_{2a}sin\varphi_2}{p_{1a}cos\varphi_1 + p_{2a}cos\varphi_2} \end{cases} \tag{3}$$

The sound pressure amplitude of the composite sound wave depends on the phase difference $\varphi_2 - \varphi_1$ of the two sound waves, and the square of the sound pressure amplitude reflects the average sound energy density $\bar{\varepsilon}$ in the sound field.

$$\bar{\varepsilon} = \frac{p_a^2}{2\rho_0 c_0^2} \tag{4}$$

Taking the time average of the above equation yields the average energy density of the composite sound wave, i.e.,

$$\bar{\varepsilon} = \overline{\varepsilon_1} + \overline{\varepsilon_2} + \frac{p_{1a}p_{2a}}{\rho_0 c_0^2}\cos(\varphi_2 - \varphi_1) \tag{5}$$

Here, if $p_{1a} = p_{2a}$, and $\varphi_2 - \varphi_1 = \pm\pi, \pm 3\pi \ldots$ equals any odd multiple of π, then the composite sound pressure amplitude and the average sound energy density are zero, with the two sound waves canceling each other out:

$$\begin{cases} p_a = p_{1a} - p_{2a} = 0 \\ \bar{\varepsilon} = \overline{\varepsilon_1} + \overline{\varepsilon_2} - \frac{p_{1a}p_{2a}}{\rho_0 c_0^2} = \frac{p_{1a}^2}{2\rho_0 c_0^2} + \frac{p_{2a}^2}{2\rho_0 c_0^2} - \frac{p_{1a}p_{2a}}{\rho_0 c_0^2} = 0 \end{cases} \tag{6}$$

When two sound waves have equal amplitude and their phase difference is π (or any odd multiple of π), the two sound waves completely interfere with each other, resulting in a total sound pressure of 0. This means that the total sound energy density at this location is also 0, i.e., the sound energy density of the composite sound field at this location is zero.

To eliminate the noise at a certain location, a sound wave opposite to the noise can be emitted so that their phase difference is π, thereby obtaining a virtually silent zone at that location. As low-frequency sound waves have long wavelengths, ANC systems can accurately detect and cancel out such noise, giving ANC a natural advantage in dealing with low-frequency noise. By contrast, high-frequency noise, with its shorter wavelength and rapid spatial changes, poses challenges to the practical application of ANC. Since road traffic noise is primarily low-frequency, ANC technology has shown obvious advantages in this field.

3.2. Structure of the Active Noise Control System

The design and implementation of active noise control systems can take many forms, including narrowband feedforward systems, broadband feedforward systems, feedback systems, hybrid systems, and multichannel systems. Considering the system's applicability and development cost, we adopted the structure of a broadband feedforward system for the research presented in this paper, as shown in Figure 4.

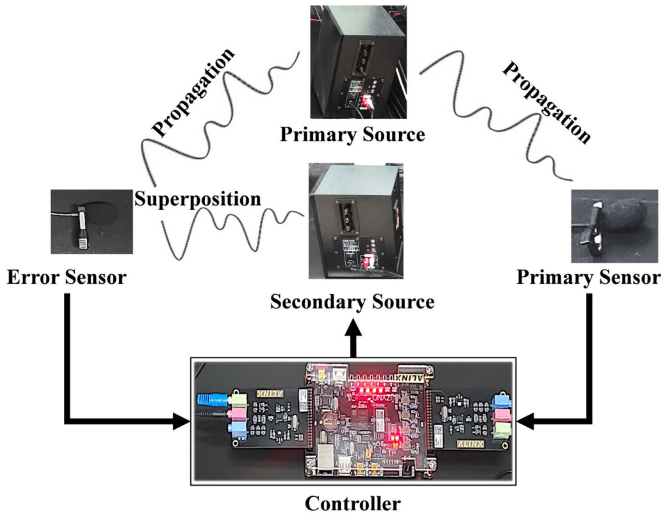

Figure 4. Schematic diagram of the broadband feedforward system [48].

The main components of the broadband feedforward active noise control system include a reference sensor, an error sensor, a secondary sound source, and a controller. The reference sensor, functioning as a non-acoustic sensor, has the primary role of predicting and capturing future noise, i.e., the reference signal. This predictive capability enables the feedforward system to respond before the noise arrives. The error sensor, typically placed in the area where noise reduction is needed, is responsible for capturing real-time noise that has not been eliminated, i.e., the so-called error signal. The controller analyzes the signals collected by the reference sensor and the error sensor, generating a signal with equal amplitude and the opposite phase to the noise to drive the secondary sound source. The secondary sound source then emits the inverse sound wave generated by the controller, interfering with the original noise to achieve noise reduction or elimination [49]. Broadband feedforward systems mainly target random broadband noises, such as traffic noise and wind noise. They rely on predicting the reference signal, which is crucial for handling non-periodic and random noise.

In the designed adaptive active noise control system, the primary path and the secondary path are key components. The primary path describes the sound propagation characteristics from the original noise source to the error sensor. Under stable environmental conditions (e.g., enclosed indoor environments), the primary path remains relatively constant. However, in practical applications, minor changes in the environment (e.g., opening windows, moving locations, the appearance of new objects, etc.) can affect the primary path. The secondary path describes the sound propagation characteristics from the secondary sound source to the error sensor. This path involves components such as D/A converters, audio filters, power amplifiers, the acoustic path from the loudspeaker to the error sensor, the error sensor itself, and A/D converters. Due to its complexity, minor changes in components or different implementation methods may cause changes in the secondary path [50,51].

3.3. Active Noise Control System Algorithm

In the realm of active noise control systems, the Least Mean Squares (LMS) algorithm holds a fundamental and crucial position among adaptive filtering algorithms. The LMS algorithm employs a steepest descent approach, recursively updating the filter coefficients. Figure 5 presents an adaptive filter model based on the LMS algorithm:

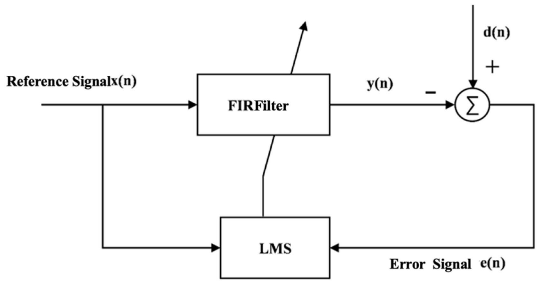

Figure 5. Adaptive filter based on Least Mean Squares (LMS) algorithm [52,53].

In this model, the reference signal $X(n)$, which represents the original noise signal, is captured by an external sensor and fed into the FIR (Finite Impulse Response) filter. This filter creates an output signal $\boldsymbol{y}(n)$ based on its weights and $X(n)$. Ideally, $\boldsymbol{y}(n)$ should match the original noise $d(n)$ in magnitude but be inversely phased for manual cancellation at the error sensor location, yielding the smallest error signal $e(n)$. The system strives to minimize $e(n)$ via continuous adaptive updates, thereby achieving optimal noise cancellation.

We first define the vector of the reference signal $X(n)$ at time n and the vector of the filter weight coefficients:

$$X(n) = [x(n), x(n-1), \ldots, x(n-L+1)]^T \tag{7}$$

$$W(n) = \left[w_0(n), w_1(n), \ldots, w_{(L-1)}(n)\right]^T \tag{8}$$

The goal is to minimize the error signal $e(n)$, the mean square value of which is:

$$E\left[e^2(n)\right] = E\left[(d(n)-y(n))^2\right] = E\left[\left(d(n)-W^T(n)X(n)\right)^2\right] \tag{9}$$

Next, we need to find the filter coefficients that minimize the mean square value, thereby minimizing the mean square value of $e(n)$ In the LMS algorithm, the steepest descent method is used; each step of the weight vector change is proportional to the negative value of the gradient vector [54], formalized as:

$$W(n+1) = W(n) - \mu\nabla(n) \tag{10}$$

Here, $\nabla(n)$ denotes the gradient vector of the nth iteration, and μ represents the iteration step size. The gradient vector is calculated as

$$\nabla(n) = \frac{\partial E\left[e^2(n)\right]}{\partial W(n)} = -2E[e(n)X(n)] \tag{11}$$

Taking the gradient of a single sample $e^2(n)$ as an estimate of the mean square error gradient, we obtain the gradient estimate:

$$\hat{\nabla}(n) = \frac{\partial e^2(n)}{\partial W} = -2e(n)X(n) \tag{12}$$

Since the gradient estimate $\hat{\nabla}(n)$ is an unbiased estimation of the real gradient $\nabla(n)$, it can replace the real gradient in Equation (10), leading to the filter weight update formula:

$$W(n+1) = W(n) - \mu\hat{\nabla}(n) = W(n) + 2\mu e(n)X(n) \tag{13}$$

To ensure the system stability, the range of the iteration step size μ must be restricted. According to the requirements of the LMS algorithm, the iteration step size should be:

$$0 < \mu < \frac{1}{\lambda_{max}} \tag{14}$$

where λ_{max} is the largest eigenvalue of the autocorrelation matrix R of the reference signal.

The steps for the broadband feedforward LMS algorithm are summarized as follows: (1) The reference sensor captures the reference signal $\boldsymbol{X}(\boldsymbol{n})$ and feeds it into the adaptive filter. The error sensor collects the error signal $\mathrm{e}(\boldsymbol{n})$ at the noise cancellation point and feeds it into the adaptive filter. (2) The adaptive filter uses the reference signal $\boldsymbol{X}(\boldsymbol{n})$ and the error signal $\mathrm{e}(\boldsymbol{n})$ to update the filter weight $\boldsymbol{W}(\boldsymbol{n})$, according to Equation (13). (3) The updated filter weight is used to generate a new output signal $\boldsymbol{y}(\boldsymbol{n})$, and at the start of the next time step, steps 1 and 2 are repeated [55,56]. Using continuous adaptive updates, we can effectively reduce the noise.

3.4. Hardware Platform Construction

The active noise control prototype system is composed of a field-programmable gate array (FPGA) development board, two audio modules, a reference sensor, an error sensor, and an active loudspeaker. The overall design is depicted in Figure 6, with a detailed breakdown of the hardware components presented in Table 1.

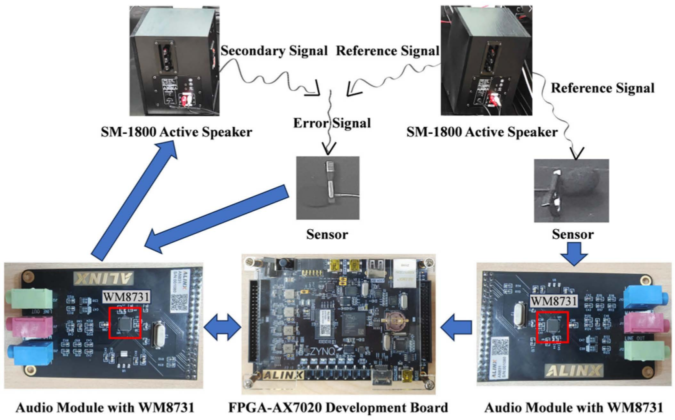

Figure 6. Hardware platform design of active noise control prototype system.

In the operation of the system, the reference sensor is placed close to the noise source to collect the reference signal, and the error sensor is placed in the noise cancellation area to collect the error signal. Each sensor is connected to the audio input interface of the respective audio module, enabling real-time signal transmission. The audio module performs analog-to-digital conversion and filtering amplification before transmitting the signal to the FPGA for algorithm analysis. The resultant secondary source signal, after the audio module's digital-to-analog conversion and filtering amplification, is transmitted to the active loudspeaker. The secondary source sound wave emitted by the active loudspeaker cancels the noise source sound wave in the noise cancellation area, reducing the noise level in the desired area.

Table 1. The hardware description of active noise control prototype system.

Hardware	Model	Manufacturer	Specifications	Function
FPGA Development Board	AX7020	Alinx Electronic Technology (Shanghai, China) Co., Ltd.	85,000 logic units, 220 multipliers	Code debugging and system control
Audio Module	WM8731	Cirrus Logic Inc. (Austin, TX, USA)	Sample rate: 8–96 KHz, data length: 16–32 bit	Audio decoding, analog-to-digital conversion
Reference Sensor	Microphone	Shenzhen Huayun Ziyuan Electronics Co., Ltd. (Shenzhen, China)	Frequency response range: 20 Hz–20 kHz, 3.5 mm audio jack, unidirectional	Noise acquisition at source
Error Sensor				Noise acquisition in the cancellation area
Active Loudspeaker	SM-1800	Feixinyuan Audio Company. (Beijing, China)	Frequency response range: 20 Hz–20 kHz	Secondary source of in the cancellation area

3.5. System Software Development

Upon finalizing the hardware selection, a software system is needed to drive the hardware platform and achieve functionalities such as audio signal transmission and algorithm execution.

(1) FPGA Development Tools and Language

This study used the Vivado 2018.3 software for development. Vivado is one of the primary development tools for FPGAs, supporting various data input methods, integrated synthesizers, and simulators. It can complete the full development process from new project design input to generating bitstream for FPGA download. The development process utilized Verilog HDL, a hardware description language that supports hardware development, verification, synthesis, and testing functions. The related active noise control algorithms can be implemented using Verilog HDL. Notably, compared to hardware filters, FPGA multi-stage adaptive filters implemented via software demonstrate greater flexibility and stability.

(2) Audio Data Interaction and Processing

The audio data interaction between the WM8731 audio decoding chip and the FPGA main chip is achieved via two serial pins, ADCDAT and DACDAT, necessitating data parallelization. As shown in Figure 7, the data transmission and processing of noise signals include the following steps.

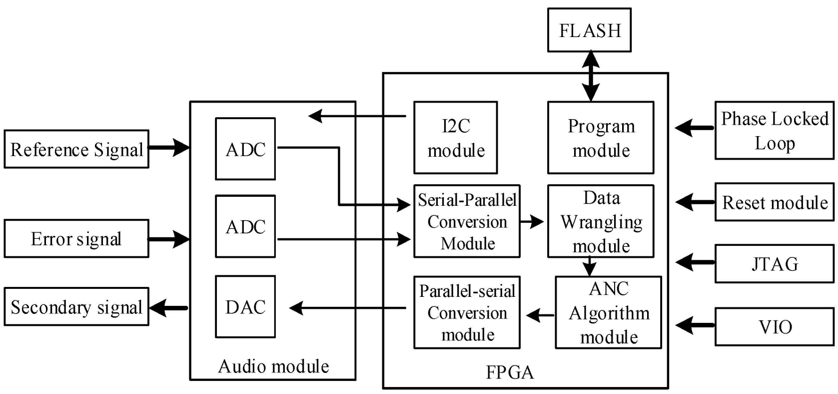

Figure 7. Noise signal data transmission and processing.

Initially, the FPGA development board configures the WM8731 audio chip's sampling rate, data format, and conversion initiation functions using the I2C configuration module, setting the sampling rate at 48 KHz, and data length for conversion at 16 bits. Next, the WM8731 chip employs the ADC conversion module to transform the analog signal collected by the sensor into a digital signal, inputting this into the FPGA's serial-to-parallel conversion module. This module then transforms the input serial digital signal into parallel

16-bit data and inputs it into the data reorganization module. After undergoing de-zeroing and redundancy removal in this module, the data are input into the ANC algorithm module.

The ANC algorithm module employs the Least Mean Squares (LMS) algorithm, a commonly used adaptive filtering algorithm suitable for processing signals with unknown attributes. The calculated secondary source signal is sent to the parallel-to-serial conversion module, which transforms the parallel data back into serial data and sends it to the WM8731 chip to complete the digital-to-analog conversion. Finally, the active speaker emits the secondary source audio, completing the active noise control.

(3) Control Program and Debugging

In the overall system, FLASH is primarily used for control program storage, while the JTAG interface is used for program debugging and burning. These two elements jointly ensure the system's stable operation and effective debugging.

4. Single- and Dual-Frequency Noise Reduction Tests

4.1. Methodology

The developed active noise control (ANC) prototype system consists of a reference speaker, a controller, a secondary source speaker, and an error sensor. The experimental design is illustrated in Figure 8.

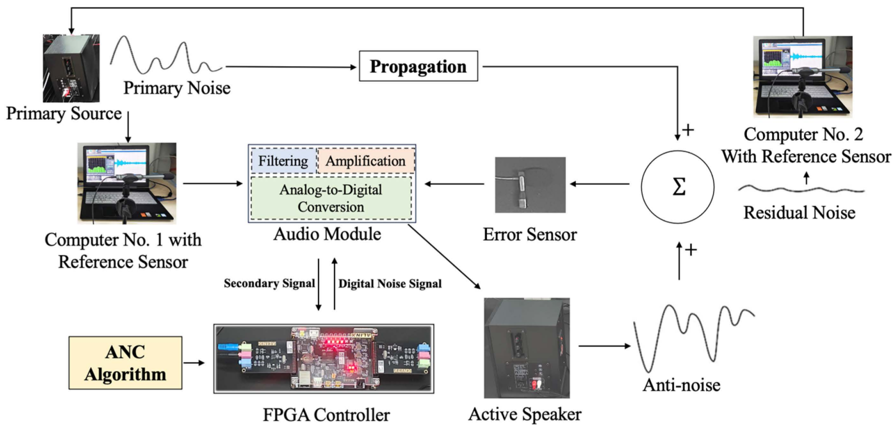

Figure 8. Schematic diagram of the developed active noise control system test.

To evaluate the performance of the ANC system, we conducted comparative indoor tests following these steps:

(1) Program Burn-in: The computer is connected to the controller through a simulator for program burn-in. Once the program is burned in, the controller can operate independently from the computer. During this time, the lab environment is kept quiet to prevent irrelevant noise from affecting the test results.

(2) Environmental Noise Measurement: A UMIK-1 measuring microphone connected to the first computer is used, with the REW V5.20.3 software (a professional acoustics measuring and analysis tool) recording the noise data throughout the experiment. Firstly, we measure and record the environmental noise in the laboratory. Before the measurement, all other devices are switched off to avoid interference.

(3) Sound Pressure Level Measurement: With the ANC system turned off, the UMIK-1 microphone is combined with the error sensor to measure the sound pressure level of the area to be silenced. The primary source speaker is connected to the second computer, using the REW V5.20.3 software to generate simulated noise sources of different frequencies. For convenience of comparison, the volume of the primary source speaker is adjusted so that the sound pressure level measured at the microphone is always maintained at 70 dBA.

(4) Observation of Noise Reduction Effect and Parameter Adjustment: Once the ANC system is activated, we can observe real-time noise reduction effects using the second computer. To achieve the best noise reduction effect, we adjust the iteration step size via the VIO module (a user interface for controlling system parameters), modify the program

to adjust the filter order, and change the distance between the primary source, reference speaker, secondary source, and error sensor to obtain the optimal parameter combination. The presented measurements are from multiple tests, and we selected the results with the best noise reduction effect.

(5) Comparison of Test Results: Finally, we compare the sound pressure level data of the area to be silenced before and after turning on the ANC system to assess the effectiveness of the ANC system.

4.2. Single-Frequency Test Result Analysis

In line with our previous research, we observed commonalities in the overall noise from different types of roads and vehicles. Peak effects surfaced within the frequency ranges of 50–80 Hz, 200–315 Hz, and 800–1250 Hz. Thus, our noise reduction tests targeted the frequency bands of 200 Hz, 500 Hz, 800 Hz, 1000 Hz, and 1200 Hz.

Given the finite speed of sound propagation, it is necessary for the sound waves emitted by the secondary source to meet the noise at the correct time and place to effectively cancel out the noise. Therefore, before starting the tests, we first adjusted the distances between the various components of the active noise control system—primary source, secondary source, reference sensor, and error sensor—to identify the relative positions that yield the maximum noise reduction [57]. Furthermore, due to the varying wavelengths and phases of sound waves at different frequencies, the optimal distances between the components for effective phase cancellation (i.e., noise reduction) will differ.

With the primary source set at 70 dBA and the indoor ambient noise at 39.2 dBA, for each test frequency, we iteratively adjusted the distances between the primary source, secondary source, and reference sensor to ascertain the positions that produced the maximum noise reduction. Multiple noise reduction tests were conducted at these positions, and the results showed that each test was very close in outcome. Hence, the median of these test results was selected for comparative analysis, as shown in Figure 9. Figure 10 presents a comparison of the spectral data before and after the activation of the active noise control system at 500 Hz.

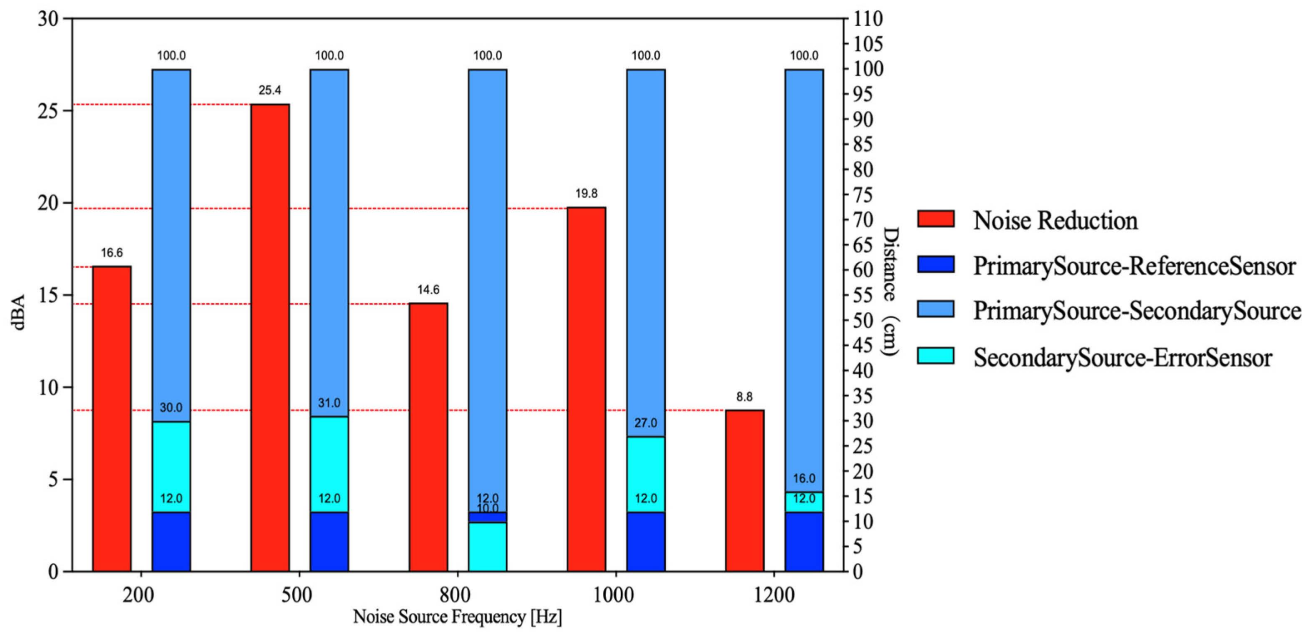

Figure 9. Maximum noise reduction and relative positions under different frequency noise.

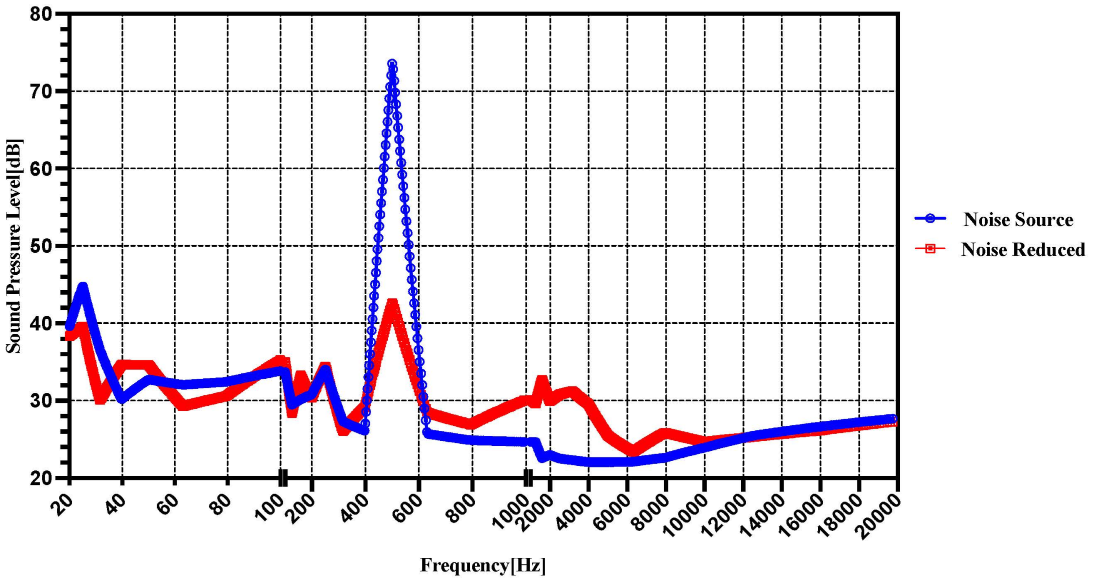

Figure 10. Single-frequency test results.

As demonstrated in Figure 10, the active noise control system provided significant noise reduction for single-frequency noise, with a reduction of around 20 dBA. Notably, the 500 Hz noise saw the most significant reduction, at 25.4 dBA, bringing the noise level in the target area close to the ambient noise level. The least reduction was seen at 1200 Hz, which decreased by 8.8 dBA.

Using testing, we observed that the noise reduction performance for extremely low or high frequencies was relatively inferior. Although theoretically lower-frequency noise should be easier to reduce, the actual noise reduction effect was hindered due to the poor frequency response of the speaker at lower frequencies. On the other hand, the real-time requirements of the active noise control system are higher for higher-frequency noise, which also impacted the noise reduction effect. These findings indicate a close relationship between the noise reduction effect of the active noise control system and the choice of hardware and software configuration.

4.3. Dual-Frequency Test Result Analysis

To evaluate the performance of our active noise control system under more complex acoustic signals, we tested it using two specific dual-frequency noise sources, 100 Hz + 1000 Hz and 200 Hz + 1000 Hz, with reference to the frequency range where traffic noise spikes occur. Following the experimental steps outlined earlier, we identified the distances that yielded the best noise reduction results and represented them in Figure 11.

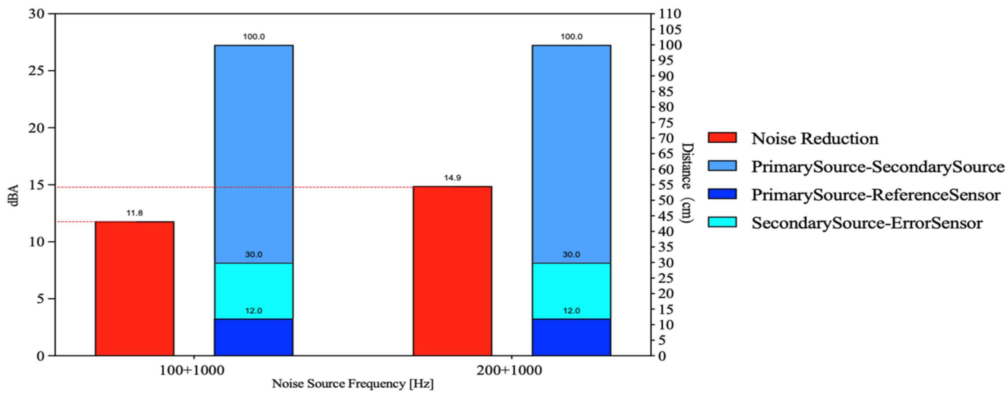

Figure 11. Maximum noise reduction and relative positions under different dual-frequency noise.

As per the results shown in Figure 12, notable noise reduction was observed at both frequencies when the noise source was 200 Hz + 1000 Hz, with an approximate reduction of 15 dB(A). However, when the noise source was 100 Hz + 1000 Hz, we noticed a significant noise reduction at 1000 Hz, but the noise reduction at 100 Hz was less pronounced.

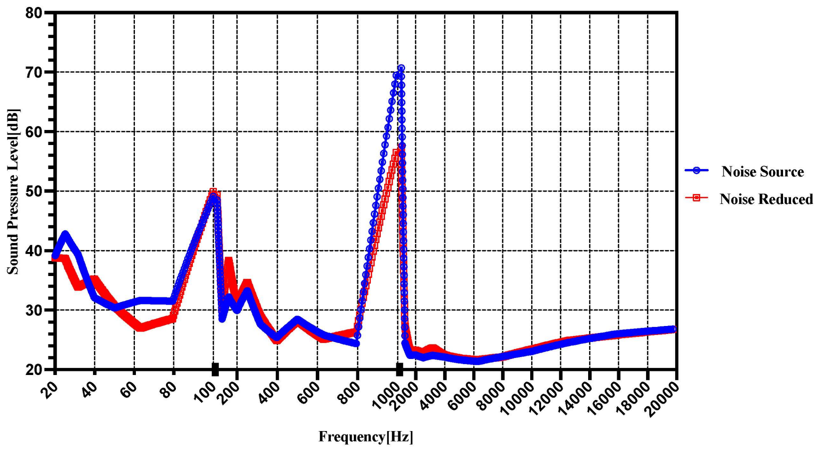

(**a**)

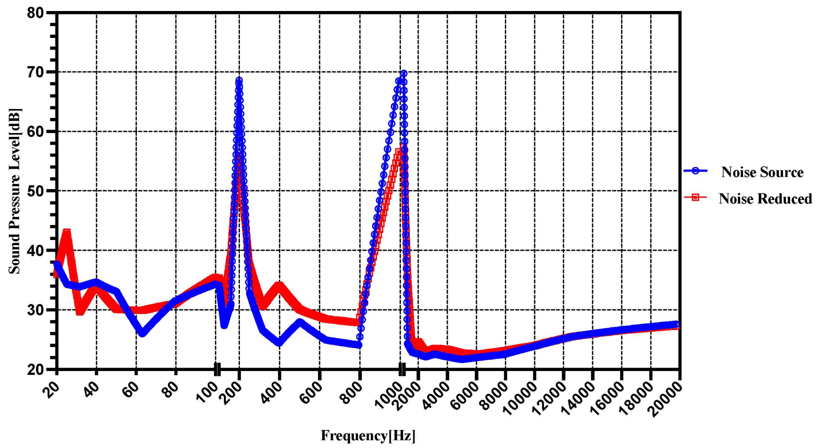

(**b**)

Figure 12. Dual-frequency test results. (**a**) Comparison for 100 Hz + 1000 Hz. (**b**) Comparison for 200 Hz + 1000 Hz.

Before the system was turned on, the sound pressure level at 100 Hz was distinctly lower than 70 dB(A). This result further confirmed the crucial impact of the sound system configuration on the effectiveness of active noise control. Factors such as the frequency response range of the sound system and gain settings could influence the performance of noise reduction. Hence, we suggest optimizing the relevant configurations of the sound system—for instance, expanding the frequency response range and adjusting gain settings—to achieve superior noise reduction outcomes.

5. Discussion

In active noise control tests for single- and dual-frequency noise, the system demonstrated significant noise reduction within the primary frequency range of road traffic noise. Moreover, it exhibited fast convergence, stable operation, and strong versatility. This paves the way for the potential application of active noise control technology in the realm of road traffic. In tests with actual road traffic noise, we did not observe significant noise reduction. However, it clearly identified the issues that need to be addressed in future research:

(1) The active noise control system failed to achieve significant noise reduction when dealing with actual road traffic noise. This could be attributed to factors such as traffic

volume, vehicle types, speed, etc., leading to the complexity of the primary and secondary path parameters and diversity in noise frequency components. For instance, heavy vehicles might produce more low-frequency noise, while motorcycles might generate more high-frequency noise. These variations could lead to changes in the primary path parameters, secondary path parameters, etc., and with each vehicle serving as a noise source, different noise sources might interfere with each other, making sound wave prediction and cancellation more complex.

(2) It was found that the speakers and sensors had poorer frequency response to low-frequency noise, which may prevent the system from accurately generating and measuring low-frequency noise, thereby affecting the accuracy of noise reduction. Similarly, due to the hardware system's latency, real-time processing of high-frequency noise also faces challenges, potentially leading to phase shifts and noise increase.

(3) In the active noise control system, electronic devices, wiring, and acoustical factors between the secondary source and the error sensor might cause latency issues. These issues have not been fully considered in the current LMS algorithm, thus affecting the noise reduction performance. Moreover, because road traffic noise is broadband noise with a wide frequency distribution, this leads to a situation in the LMS algorithm where the larger the frequency range of the input signal, the higher the signal correlation, and the slower the algorithm converges, thereby affecting the noise reduction effect.

To adapt to the characteristics of road traffic noise, future research could be based on the theory of reference sub-band filtering to improve the algorithm's convergence speed and noise reduction effect by processing the input signal into several narrow-band noise signals. Consideration could also be given to enhancing the hardware performance of the sensors and speakers, such as improving the sensor signal-to-noise ratio, speaker frequency response characteristics, controller computational speed, system integration, and stability, especially assessing the active noise control performance of speakers in the low-frequency range. Further exploration of active noise control applications in the traffic domain can also be carried out, including a combination with passive technologies such as noise barriers and research into active noise control technology for vehicle tire–road noise.

6. Conclusions

A thorough analysis of the characteristics of various types of road traffic noise was conducted in this study, culminating in the successful development of a prototype for an active noise control system specifically targeting road traffic noise. Active noise control tests were performed in a lab environment, and the results indicated that the system could effectively reduce single-frequency and dual-frequency noise. This suggests innovative ideas and strategies for the application of active noise control technology in road traffic noise management. The main findings are as follows:

(1) Field traffic noise tests were conducted using a self-assembled noise collection and analysis system. The type and speed of vehicles were found to significantly impact the overall traffic noise produced. However, the mixed traffic noise typically lies within the range of 50–80 Hz, 200–315 Hz, and 800–1250 Hz.

(2) For different types of vehicles, when the speed exceeds 40 km/h, the traffic noise generated by small vehicles is concentrated around 1000 Hz, medium vehicles around 500 Hz, and large vehicles around 63 Hz.

(3) An active noise control prototype system based on a FPGA was constructed, and ingle-frequency and dual-frequency noise reduction tests were performed. The noise reduction effect was found to be satisfactory for single-frequency noise. When the noise frequency was 500 Hz, it could be reduced by nearly 30 dBA. For dual-frequency noise, at 200 Hz + 1000 Hz, a reduction of 15 dBA was achieved.

Author Contributions: All authors contributed significantly to the work presented in this manuscript. J.Y., B.Y. and L.W. designed and performed the experiments; B.Y., J.Y., Z.Y. and S.Y. analyzed the data and wrote this manuscript; B.Y. and L.W. provided valuable advice and contributions. All authors have read and agreed to the published version of the manuscript.

Funding: This work was supported by the Technology Innovation and Demonstration Project of the Department of Transport of Yunnan Province (2021) no. 25, funded by the Department of Transport of Yunnan Province. This work was also supported by the National Natural Science Foundation of China (no. 52208414).

Data Availability Statement: The data presented in this study are available on request from the corresponding author. The data are not publicly available due to the confidentiality requirements of the project.

Conflicts of Interest: Author Biyu Yang was employed by the company Zhaotong Highway Investment Development Co., Ltd. The remaining authors declare that the research was conducted in the absence of any commercial or financial relationships that could be construed as a potential conflict of interest.

References

1. Carter, N.L. Transportation noise, sleep, and possible after-effects. *Environ. Int.* **1996**, *22*, 105–116. [CrossRef]
2. Öhrström, E.; Skånberg, A.; Svensson, H.; Gidlöf-Gunnarsson, A. Effects of road traffic noise and the benefit of access to quietness. *J. Sound Vib.* **2006**, *295*, 40–59. [CrossRef]
3. Moon, H.R.; Shon, J.G. A study on the characteristics of applicability in the active noise cancellation system and measurement of the road noise for traffic calming. *Trans. Korean Inst. Electr. Eng. P* **2013**, *62*, 111–116. [CrossRef]
4. Zhang, X.J. Study on the formwork support and pouring technology of fully enclosed sound barrier construction. *J. Munic. Technol.* **2023**, *41*, 219–224.
5. Rawool, S.; Stubstad, R. Effect of diamond grinding on noise characteristics of concrete pavements in California. In Proceedings of the National Conference on Preservation, Repair, and Rehabilitation of Concrete Pavements, St. Louis, MO, USA, 22–24 April 2009.
6. Xu, J.; Yang, S.L.; Ye, Z.J.; Wang, L.B.; Wei, Y.; Yang, B.Y.; Meng, W.; Cui, T.; He, C.W. Analysis of driving noise characteristics on cement concrete pavement with different groove textures. *J. Munic. Technol.* **2023**, *41*, 27–35.
7. Liu, J.; Li, J.; Li, X.Y.; Li, M.L. Determination of elastic component amounts of perforated elastic road surface and analysis of the noise reduction effect. *J. Munic. Technol.* **2023**, *41*, 7–11.
8. Shen, J.; Zhang, Y.D.; Huang, C.; Liu, W.; Zhao, X.T.; Hu, K.Z. Application of double-layer porous asphalt in urban extra-long tunnel. *J. Munic. Technol.* **2022**, *40*, 40–46.
9. Jiang, T.H.; Ren, W.Y.; Dong, Y.S.; Hou, Y.; Yuan, J.M. Precise representation of macro-texture of pavement and effect on anti-skidding performance. *Munic. Eng. Technol.* **2022**, *40*, 24.
10. Lu, L.; Yin, K.-L.; de Lamare, R.C.; Zheng, Z.; Yu, Y.; Yang, X.; Chen, B. A survey on active noise control in the past decade—Part I: Linear systems. *Signal Process.* **2021**, *183*, 108039. [CrossRef]
11. Huang, Y.; He, S.L.; Xu, H.T.; Li, W.P. Research on Activate Noise Control in Head Space of EVA Spacesuit. *Manned Spacefl.* **2023**, *29*, 186–191.
12. Zhang, L.M.; Qiu, X.J. Causality study on a feedforward active noise control headset with different noise coming directions in free field. *Appl. Acoust.* **2014**, *80*, 36–44. [CrossRef]
13. Zhang, L.M.; Tao, J.C.; Qiu, X.J. Active control of transformer noise with an internally synthesized reference signal. *J. Sound Vib.* **2012**, *331*, 3466–3475. [CrossRef]
14. Pan, M. Adaptive Control of a Piezoelectric Valve for Fluid-Borne Noise Reduction in a Hydraulic Buck Converter. *J. Dyn. Syst. Meas. Control.* **2017**, *139*, 081007. [CrossRef]
15. Sun, Y.P.; Sun, H.L.; Zhang, W.; Wang, H.; Yang, J. Experimental research into active control of low-frequency line spectral disturbances in liquid-filled pipe. *J. Chin. J. Ship Res.* **2017**, *12*, 122–127.
16. Zhang, S.R. Application Research of Mine Active Noise Control Technology. *Min. Saf. Environ. Prot.* **2016**, *43*, 4.
17. Liu, X.J.; Zhao, C.; Lei, J.U.; Jun-Cheng, X.U.; Jiang, Y. The secondary path modeling for fMRI scanning noise active control system. *Chin. J. Magn. Reson. Imaging* **2018**, *9*, 8.
18. Reddy, R.M.; Panahi, I.M.; Briggs, R. Hybrid FxRLS-FxNLMS Adaptive Algorithm for Active Noise Control in fMRI Application. *IEEE Trans. Control. Syst. Technol.* **2011**, *19*, 474–480. [CrossRef]
19. Xu, G.G.; Lu, X.; Shi, C.L.; Zhu, Y.G.; Zheng, S. Application of road surface recognition technology in the optimization of noise reduction performance of active road noise control. *J. Chongqing Univ. Technol. (Nat. Sci.)* **2022**, *36*, 74–81.
20. Feng, T.; Sun, G.H.; Li, M.F.; Lim, T.C. Multi-Reference Time-Frequency Active Control of Vehicle Interior Road Noise. In *Structural Health Monitoring, Damage Detection & Mechatronics, Volume 7: Proceedings of the 34th IMAC, A Conference and Exposition on Structural Dynamics 2016*; Springer: Cham, Switzerland, 2016; pp. 121–128.

21. Zhang, S.; Zhang, L.; Meng, D.; Pi, X. Active control of vehicle interior engine noise using a multi-channel delayed adaptive notch algorithm based on FxLMS structure. *Mech. Syst. Signal Process.* **2023**, *186*, 109831. [CrossRef]
22. Jiang, H.B.; Zhang, Q.F. Research on active noise reduction technology in vehicle based on improved SPSA algorithm. *Agric. Equip. Veh. Eng.* **2023**, *61*, 76–80.
23. Zhang, L.J.; Ning, Y.B.; Meng, D.J.; Zhang, S. Method of Constructing Virtual Reference Signals Utilizing Grouping for Active Road Noise Control in Vehicles. *J. Tongji Univ. (Nat. Sci.)* **2021**, *49*, 712–720.
24. Landaluze, J.; Portilla, I.; Pagalday, J.; Martınez, A.; Reyero, R. Application of active noise control to an elevator cabin. *Control. Eng. Pract.* **2003**, *11*, 1423–1431. [CrossRef]
25. Guo, J.; Sun, K.; Wang, C.-S.; Fang, S.-P.; Horie, Y.; Yang, J.-Y.; Liu, Y.-Y.; Wang, F.; Liu, L.-Y.; Fan, J.-Y.; et al. Protective effects of dihydroxylphenyl lactic acid and salvianolic acid B on LPS-induced mesenteric microcirculatory disturbance in rats. *Shock* **2008**, *29*, 205–211. [CrossRef] [PubMed]
26. Zhang, X.F. Research on Sound Field Distribution of Active Control of Low-Frequency Traffic Noise in Highway Tunnel. Ph.D. Thesis, Beijing Jiaotong University, Beijing, China, 2018.
27. Moon, H.R.; Kim, S. A Basic Lab Study for the Road Application of the Active Noise Reduction Technology. *ATZ Worldw.* **2016**, *120*, 38–43.
28. Lu, L.; Yin, K.-L.; de Lamare Rodrigo, C.; Zheng, Z.S.; Yu, Y.; Yang, X.; Chen, B. A survey on active noise control in the past decade–Part II: Nonlinear systems—ScienceDirect. *Signal Process.* **2020**, *181*, 107929. [CrossRef]
29. Lam, B.; Gan, W.S.; Shi, D.; Nishimura, M.; Elliott, S. Ten questions concerning active noise control in the built environment. *Build. Environ.* **2021**, *200*, 107928. [CrossRef]
30. Hart, C.R.; Lau, S.K. Active noise control with linear control source and sensor arrays for a noise barrier. *J. Sound Vib.* **2012**, *331*, 15–26. [CrossRef]
31. Duhamel, D.; Sergent, P.; Hua, C.; Cintra, D. Measurement of active control efficiency around noise barriers—ScienceDirect. *Appl. Acoust.* **1998**, *55*, 217–241. [CrossRef]
32. Sahib, M.A.; Streif, S. Design of an active noise controller for reduction of tire/road interaction noise in environmentally friendly vehicles. In Proceedings of the 2017 Signal Processing: Algorithms, Architectures, Arrangements, and Applications (SPA), Poznan, Poland, 20–22 September 2017; IEEE: New York, NY, USA, 2017.
33. Zhang, C.; Qin, M.; Zou, H.; Qiu, X. *Secondary Source and Error Sensing Strategies for the Active Control of Sound Transmission through a Small Opening*; Academic Press: Cambridge, MA, USA, 2020.
34. *GB3096-2008*; Ministry of Ecology Environment of the People's Republic of China: Environmental Quality Standard for Noise. China Environmental Science Press Beijing: Beijing, China, 2008.
35. *HJ 460-2012*; Ministry of Environmental Protection of the People's Republic of China: Technical Specifications for Environmental Noise Monitoring Routine Monitoring for Urban Environmental Noise. China Environmental Science Publishing House: Beijing, China, 2012.
36. Li, T. Literature review of tire-pavement interaction noise and reduction approaches. *J. Vibroeng.* **2018**, *20*, 2424–2452. [CrossRef]
37. Ruhala, R.J.; Burroughs, C.B. Localization of tire/pavement noise source regions. *Noise Control. Eng. J.* **2008**, *56*, 318–331. [CrossRef]
38. Ongel, A.; Harvey, J. Pavement characteristics affecting the frequency content of tire/pavement noise. *Noise Control. Eng. J.* **2010**, *58*, 563–571. [CrossRef]
39. Ling, S.; Yu, F.; Sun, D.; Sun, G.; Xu, L. A comprehensive review of tire-pavement noise: Generation mechanism, measurement methods, and quiet asphalt pavement. *J. Clean. Prod.* **2021**, *287*, 125056. [CrossRef]
40. Rasmussen, R.O.; Sohaney, R.C. *Tire-Pavement and Environmental Traffic Noise Research Study*; DTD Applied Research and Innovation Branch: Denver, CO, USA, 2012.
41. Luo, P.; Cai, M.; Wang, H.B. Frequency Characteristics of Noises of Various Types of Vehicles in Different Speeds. *J. Noise Vib. Control.* **2013**, *33*, 86.
42. Bocharov, A.A.; Kolesnik, A.G.; Soloviev, A.V. Two-parametric model of the spectrum of traffic noise in Tomsk. *Acoust. Phys.* **2012**, *58*, 718–724. [CrossRef]
43. Nunez, I.G.C.; Miranda, J.G.O.; Duarte, M.V. Active noise control in acoustic shutters. *Appl. Acoust.* **2019**, *152*, 41–46. [CrossRef]
44. Piechna, J. A Review of Active Aerodynamic Systems for Road Vehicles. *Energies* **2021**, *14*, 7887. [CrossRef]
45. Song, L.Z.; Feng, Q.S.; Sun, K.; Liu, Q.; Luo, Y. Test on vibration noise of rail corrugation section on urban rail transit viaduct. *J. Traffic Transp. Eng.* **2021**, *21*, 159–168.
46. Guo, Z.; Yi, J.; Xie, S.; Chu, J.; Feng, D. Study on the Influential Factors of Noise Characteristics in Dense-Graded Asphalt Mixtures and Field Asphalt Pavements. *Shock Vib.* **2018**, *2018*, 5742412. [CrossRef]
47. Zhao, H.P.; Zhou, Y.L.; Zhang, Q.Z. Active Noise Control with Double Channels Based on Virtual Sensors. *J. Electroacoust.* **2010**, *34*, 79–84+87.
48. Zhang, S.; Zhang, L.; Meng, D.; Zhang, X. A hybrid feedforward/feedback multi-channel active control system with optimization for cancelling road noise inside a vehicle cabin. *Appl. Acoust.* **2022**, *201*, 109128. [CrossRef]
49. Park, Y.S.; Cho, M.H.; Oh, C.S.; Kang, Y.J. Coherence-based sensor set expansion for optimal sensor placement in active road noise control. *Mech. Syst. Signal Process.* **2022**, *169*, 108788. [CrossRef]

50. Yin, L.; Zhang, Z.; Wu, M.; Wang, Z.; Ma, C.; Zhou, S.; Yang, J. Adaptive parallel filter method for active cancellation of road noise inside vehicles. *Mech. Syst. Signal Process.* **2023**, *193*, 110274. [CrossRef]
51. Jung, W.; Elliott, S.J.; Cheer, J. Local active control of road noise inside a vehicle. *Mech. Syst. Signal Process.* **2019**, *121*, 144–157. [CrossRef]
52. George, N.V.; Panda, G. Advances in active noise control: A survey, with emphasis on recent nonlinear techniques. *Signal Process.* **2013**, *93*, 363–377. [CrossRef]
53. Jia, Z.; Zheng, X.; Zhou, Q.; Hao, Z.; Qiu, Y. A Hybrid Active Noise Control System for the Attenuation of Road Noise Inside a Vehicle Cabin. *Sensors* **2020**, *20*, 7190. [CrossRef] [PubMed]
54. Zhu, L.; Qiu, X.; Mao, D.; Wu, S.; Zhong, X. Efficient segment-update block LMS-Newton algorithm for active control of road noise. *Mech. Syst. Signal Process.* **2023**, *198*, 110436. [CrossRef]
55. Oh, C.S.; Ih, K.D.; Lee, H.M.; Jeon, J.S. Development of an active road noise control system. *ATZ Worldw.* **2015**, *117*, 36–39. [CrossRef]
56. Chen, M.X.; Zhou, Y.L.; Zhang, Q.Z. Directional weighted filter with 12 directions to remove random valued impulse noise. *Appl. Res. Comput.* **2014**, *31*, 1584–1587.
57. Cheer, J.; Elliott, S.J. Active noise control of a diesel generator in a luxury yacht. *Appl. Acoust.* **2016**, *105*, 209–214. [CrossRef]